Anomalous Aging of EPDM and FEPM under Combined Thermo-Oxidative and Hydrolytic Conditions

Erica M. Redline†[a], Mathias C. Celina†, Charles E. Harris†, Nicholas H. Giron†, Toshifumi Sugama‡, Tatiana Pyatina‡

†Sandia National Laboratories

Organic Materials Science Department

PO Box 5800

Albuquerque NM 87185

[a] Corresponding author: emredli@sandia.gov; (505) 845-9161

‡Sustainable Energy Technologies Department

Brookhaven National Laboratory

Upton, NY 11973-5000

Abstract:

Previous observation of EPDM and FEPM materials aged in thermo-oxidative and thermo-oxidative plus hydrolytic environments revealed an unusual trend: the degradation and disintegration of these polymers in the former case but the ability to maintain mechanical performance and shape in the latter [1]. No abnormalities were observed in the chemical (oxidation rates, FTIR spectra, solvent uptake, gel content, and weight loss vs. temperature) or physical (modulus profile) measurements that could explain these empirically observed aging differences. A second controlled aging test was conducted to verify this trend using only EPDM. Once again it was shown that thermo-oxidative conditions appear to cause more degradative damage (enhanced embrittlement) than observed for the combined thermo-oxidative coupled with hydrolytic environments. From these data we conclude that water may favorably interfere with normal thermo-oxidative degradation processes. This interference may occur via some type of inhibition pathway possibly linked to pH and hydroperoxide stability against peroxy anion formation, or through other processes that result in oxidation rate and O_2 permeability changes or yield additional sensitivity to hydrolytic damage which could counteract oxidatively induced material hardening.

Key Words: Polymer Degradation; High Temperature; Steam Environment; Mechanistic Changes; Anomalous Aging

1. Introduction:

In our previous publication,[1] we subjected several elastomers to high temperature (300°C) and high pressure (8618 kPa, 1250 psi) under oxidative plus hydrolytic conditions to simulate conditions in geothermal wells. This was the first study conducted at such high temperatures and pressures for a range of commercial elastomers. Prior degradation behavior for geothermal applications had only been studied up to 150°C [2-4]. Other pertinent studies on elastomer performance in high temperature, high pressure settings can be found in relation to their use in the oil and gas industries [5-8]. However, these previous oil and gas studies concentrated on exposure to gaseous or hydrocarbon-based environments, which is not relevant to a geothermal well where the down-hole exposures are primarily aqueous and with varied brine chemistries.

Polymer electrolyte membranes (PEM) have been investigated under acidic aqueous environments and atmospheric pressures, but only at temperatures up to 80°C [9, 10]. Furthermore, Sandia's decades-long research activities on elastomeric O-rings have primarily focused on lifetime predictions of materials at room temperature; these predictions being carried out using accelerated aging in dry conditions [11-14], not the high temperatures and aqueous surroundings of geothermal wells. Therefore, our research addresses a knowledge gap for elastomer aging behavior under combined high temperature, high pressure, thermo-oxidative and thermo-hydrolytic conditions and how this relates to lifetime predictions for commercially produced elastomers.

During the course of our study, an unexpected abnormality was observed in EPDM and FEPM O-ring aging behavior; namely, it appeared that steam interfered with oxidative degradation processes. Using ultrasensitive oxygen consumption measurements in conjunction with careful examination of spatial, physical changes (elastic modulus), we show that this anomaly is reproducible in three different EPDM formulations. Furthermore, we also discovered that the effectiveness of steam on reducing thermo-oxidative degradation was amplified as temperature was increased.

2. Experimental:

2.1 Materials

Two different elastomeric O-rings were supplied by Precision Associates, Inc.: poly(ethylene-co-propylene-co-5-ethylidene-2-norbornene, EPDM) terpolymer "70 Duro Black EPDM" and poly[tetrafluoroethylene (TFE)-co-propylene (P), FEPM] copolymer "90 Duro Black Aflas®". These O-rings were approximately one-inch in outer diameter and had a cross-section of 0.19 in. Two additional EPDM rubbers, SR793B-80 filled and unfilled, were also tested. The formulation for the filled version of SR793B-80 [15] is listed in Table 1. SR793B-80 Formulation., with the unfilled version containing no carbon black.

Table 1. SR793B-80 Formulation.

Constituent	phr
DuPont Nordel™ 1440[a]	100
Zipstick 85[b]	5
N-990 carbon black	40
N-539 carbon black	25
Flectol H[c]	2
DiCup 40C[d]	12
SR-350[e]	10

[a]*Nordel™ 1440 is a terpolymer of ethylene, propylene and 1,4 hexadiene, with an ethylene to propylene ratio of ~53 to 47 and ~3 pph of the hexadiene.*

[b]*Zipstick 85 is a zinc oxide powder.*

[c]*Flectol H is polymerized 1,2, dihydro-2,2-4-trimethyl quinolone, an antioxidant.*

[d]*DiCup 40C is a co-curing agent containing 40% dicumyl peroxide.*

[e]*SR-350 is the co-curing agent trimethylol propane trirnethacrylate.*

2.2 Thermal Aging

Thermal aging experiments were carried out at Brookhaven National Laboratory using a 2 L pressure vessel. For tests under dry (i.e. no water or steam) oxidative conditions, samples were placed in the pressure vessel, sealed, and then heated to 300°C for 24 hours, followed by a rapid (50°C/min) quench to room temperature; thermal cycling was repeated five times. Materials subjected to thermal plus hydrolytic (steam) and oxidative conditions followed the same heating

and cooling method as dry thermal cycling, with the exception that the vessel was filled to approximately 10% by volume with water and the sample suspended above the water in the headspace prior to the vessel being sealed. The final condition was thermal cycling under hydrolytic, non-oxidative conditions whereby nitrogen was purged through the top of the vessel for 10 minutes before it was sealed at atmospheric pressure and heated/cooled according to the dry oxidative conditions procedure. A summary of these aging conditions can be found in

Table 2.

Table 2. Summary of thermal aging conditions.

Condition (designation)	**Temp. (°C)**	**p_{O2}* kPa (psi)**	**p_{N2}* kPa (psi)**	**p_{H20} kPa (psi)**	**Total Pressure kPa (psi)**	**Submerged (Y/N)**
Dry, oxidative ($\Delta + O_2$)	300	41 (6)	152 (22)	-	193 (28)	N
Wet**, oxidative ($\Delta + O_2 + H_2O$)	300	41 (6)	152 (22)	8618 (1250)	8812 (1278)	N
Wet**, non-oxidative ($\Delta + H_2O$)	300	-	193 (28)	8618 (1250)	8812 (1278)	N

**Calculated based on partial pressure of the indicated gas (3.1 psi, 21 kPa, 159 torr for O_2; 11.5 psi, 79 kPa, 593 torr for N_2) in Upton, NY (~0 feet elevation) and room temperature.*

***Note: Water evaporation will reduce the initial water volume. This will somewhat lower the effective O_2 partial pressure as the total available gas volume slightly increases.*

2.3 Analysis of Chemical Changes

2.3.1 Infrared Spectroscopy

Attenuated Total Reflectance-Fourier Transform Infrared Spectroscopy (ATR-FTIR) was used to identify any oxidation derivatives that were incorporated into the elastomers exposed to the three environments as well as to assess potential alterations in chemical structures. A Bruker ALPHA ATR-FTIR spectrometer with a Ge crystal was used to collect the data. An average of 24 spectra with 4 cm^{-1} resolution was taken for each sample.

2.3.2 Thermogravimetric Analysis

Thermogravimetric analysis (TGA) was employed as a screening method for assessing the extent of material aging; this was achieved by measuring mass loss, which is an indication of volatile formation during aging/degradation processes. While elastomers are generally presumed to undergo crosslinking reactions during aging and degradation [16, 17], some materials, e.g. polypropylene, can also experience scission reactions under hydrolytic conditions [18]. These scission processes are anticipated to create weaknesses in the polymer and the subsequent formation of semi-volatile degradation products that may be picked up by a TGA screening method. For the tests, approximately 10 – 50 mg of material from the O-ring exterior was heated to 700°C in an N_2 flow at a rate of 20°C/min using a TA Instruments TGA Q50 V20.10. Note that there is a potential issue with chemical heterogeneity of the aged O-rings; sampling the exteriors was done to minimize this issue, but, nevertheless, there could be some differences in the data depending on where the sample was taken and how homogeneously it was aged.

2.3.3 Oxidation Rate Measurements

Ultrasensitive oxygen consumption rate measurements were carried out using an Oxzilla™ II respirometer with care taken to ensure non-diffusion limited oxidation (DLO) conditions at aging temperatures [19, 20]. Around 100 mg of each of the polymers were cut into a maximum of approximately one mm thick pieces and added to a 20 cc ampoule that was filled with reference air. The ampoule was placed in an oven and allowed to heat to the desired temperature before being briefly vented to return the vessel to atmospheric pressure.

2.4 Analysis of Mechanical Changes

2.4.1 Modulus Profiling

Elastic modulus profiles of aged specimen cross-sections were obtained using a customized instrument [21]. This method allows for the characterization of changes in the stiffness of the elastomers exposed to the different aging conditions. The instrument operates by scanning the surface with a parabolic tip at user-defined intervals (in this case, 0.02, 0.1, or 0.2 mm) and uses displacement from a known force applied to each point on a sample to calculate inverse tensile compliance, which is proportional to the tensile (elastic) modulus [21]. Sample preparation included cross-sectioning O-rings, embedding the materials in a suitable “soft” epoxy (ca. 5 MPa elastic modulus), and polishing with a polishing wheel to achieve a smooth surface. The embedding material was chosen as an approximate modulus match to the elastomers; this technique is preferred to prevent a rigid encapsulation material from interfering with the elastomer characterization at the epoxy/elastomer interface.

3. Results & Discussion

Our initial aging study revealed that the chosen EPDM and FEPM showed visible signs of degradation when exposed to thermal-oxidative conditions, but remained intact after subjecting it

to thermal-hydrolytic and thermal-oxidative plus hydrolytic environments (Table 3) [1]. To reiterate, each aging condition consisted of 120 hours at 300°C, with the addition of 8616 kPa (1250 psi) pressure in the cases where steam was present. This result is counterintuitive, as one would expect degradation to occur in all cases and likely to a larger extent when both oxygen and steam are present.

Table 3. Photographs showing EPDM and FEPM O-rings after aging under thermo-oxidative ($\Delta + O_2$), thermo-oxidative + hydrolytic ($\Delta + O_2 + H_2O_{(g)}$) and thermo-hydrolytic ($\Delta + H_2O_{(g)}$) conditions.

Material	**Aging Condition**		
	$\Delta + O_2$	$\Delta + O_2 + H_2O_{(g)}$	$\Delta + H_2O_{(g)}$
EPDM			
FEPM			

Characterization of the O-ring materials via ATR-FTIR spectroscopy is somewhat challenging because these elastomers are black in color. It has been suggested that non-isothermal TGA can be used as a method for determining activation energies in polymers [22, 23]. Therefore, we

utilized TGA as a first pass analysis to uncover any differences between unaged and aged O-rings (Figure 1).

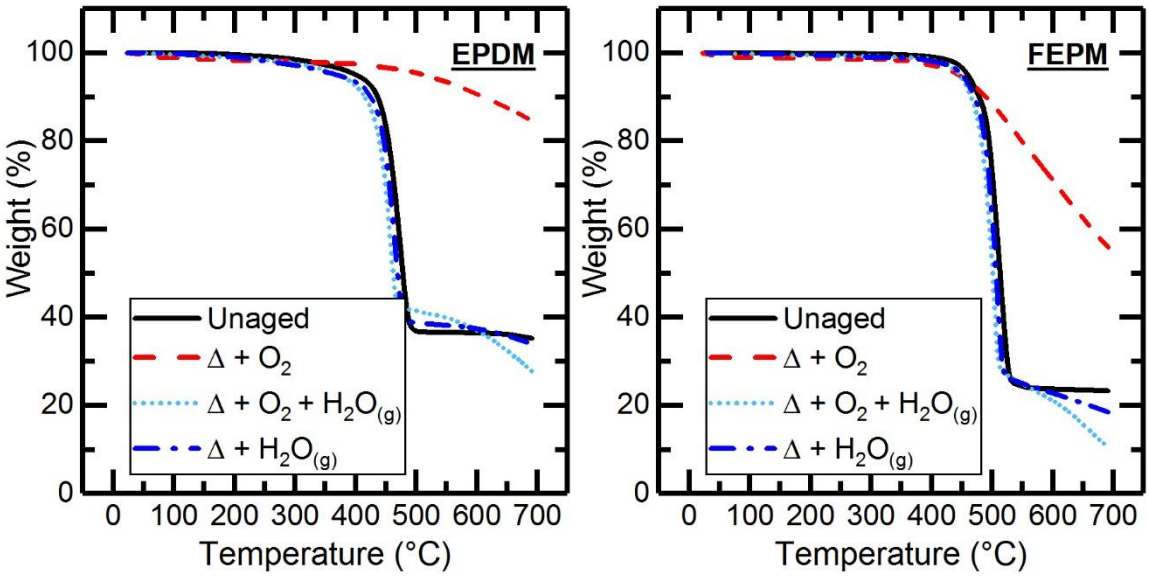

Figure 1. Weight loss as a function of temperature for (left) EPDM and (right) FEPM O-rings. The black, solid line indicates unaged materials, the dashed line represents thermal cycling in air ($\Delta + O_2$), the dotted line shows thermal cycling in air and steam ($\Delta + O_2 + H_2O_{(g)}$), and the dash-dot line depicts thermal cycling in nitrogen and steam ($\Delta + H_2O_{(g)}$). Only the $\Delta + O_2$ aged material is distinctly different in terms of its aging state.

Figure 1 data clearly demonstrate that only large changes in chemistry are discernable using our TGA method. Neither EPDM nor FEPM aged in the presence of steam show significant changes in weight-loss behavior; this is true whether the materials were aged in air ($\Delta + O_2 + H_2O_{(g)}$) or nitrogen ($\Delta + H_2O_{(g)}$). Contrarily, thermal cycling in air ($\Delta + O_2$) caused a more dramatic change in curve shape for both elastomers, likely due to the formation of carbonaceous compounds during thermo-oxidative induced aging. Since samples were taken from the exterior of the O-ring we believe this aging state does not continue to the inner portion of the O-rings, but rather is the

result of diffusion limited oxidation. The exception to this is the $\Delta + O_2$ aged EPDM, which was reduced to a powder during the aging process. Further analyses discussed below also support this conclusion.

The TGA data was additionally examined to determine the onset degradation temperature, i.e. the temperature where measurable weight loss begins, not the temperature of maximum decomposition, (Table 4). A change in the onset degradation temperature is one way to rank the O-rings in terms of damage sustained during the three different aging conditions; the lower the onset degradation temperature of the aged polymer in relation to the unaged material, the more damage the O-ring sustained. Both EPDM and FEPM followed the same ranking of least to most change in onset degradation temperature: thermo-hydrolytic ($\Delta + H_2O$) < thermo-oxidative-hydrolytic ($\Delta + O_2 + H_2O$) < thermo-oxidative ($\Delta + O_2$).

Table 4. Onset degradation temperature (temperature where ramped TGA weight loss begins - not temperature of maximum decomposition) of unaged and aged EPDM and FEPM.

Aging Condition	**EPDM Onset Degradation Temperature, °C**	**FEPM Onset Degradation Temperature, °C**
Control (unaged)	118	152
$\Delta + O_2$	29	27
$\Delta + O_2 + H_2O_{(g)}$	43	47
$\Delta + H_2O_{(g)}$	94	54

Chemical changes associated with polymer aging are often analyzed using FTIR spectroscopy [16, 17]. Oxidative damage may be assessed via the reduction or elimination of bands associated with the existing polymer chemistry, as well as with the appearance of new peaks related to oxygen-containing species, e.g. alcohols, carboxylic acids, carbonyls. Both virgin and aged materials were assessed using FTIR to ascertain differences between the spectra (Figure 2-Figure 4).

Unaged EPDM shows characteristic bands for C-H stretching, scissoring, and bending at 2800-3000 cm^{-1}, 1416 cm^{-1}, and 1377 cm^{-1}, respectively (Figure **2**). The sample aged under thermo-oxidative conditions ($\Delta + O_2$) showed a change in the ratio of the peaks at 2800-3000 cm^{-1}, 1416 cm^{-1}, and 1377 cm^{-1} as well as a significant reduction in each. Exposure to thermo-oxidative + hydrolytic aging ($\Delta + O_2 + H_2O_{(g)}$) showed oxidative products around 1715 cm^{-1}; this signal is not very strong, which may be due to the release of volatiles associated with that peak at the very high aging temperatures involved in the experiment. Additionally, spectral quality of the aged samples is poor, likely due to the black color of the sample.

The FEPM O-rings (Figure 3 and Figure 4) showed little change in the steam environments ($\Delta + O_2 + H_2O_{(g)}$ and $\Delta + H_2O_{(g)}$). On the other hand, exposure to thermo-oxidative conditions ($\Delta + O_2$) caused a dramatic spectral change, with hydrocarbon bands from 2800-3000 cm^{-1} and 1442 and 1466 cm^{-1} virtually eliminated, while the 1067 cm^{-1} peak associated with fluorocarbon stretching was also dramatically reduced.

Figure 4 spectra were normalized to the unaged C-F peak at 1067 cm^{-1}; the peak height pertaining to the $C\text{-}CH_2$ scissor and $C\text{-}CH_3$ bend, 1442 and 1466 cm^{-1}, respectively, of these normalized spectra coincidentally correlated with the TGA ordering of damage by aging condition. Namely, the most damage (largest reduction in peak height) was observed with $\Delta + O_2$

exposure and the least with $\Delta + H_2O_{(g)}$. This figure also shows evidence of diffusion limited oxidation (DLO), whereby the interiors of the samples display less degradation than the exterior. In fact, all of the aged material interiors are approximately the same peak height at 1442 and 1466 cm^{-1}. Finally, the significant spectral changes of EPDM and FEPM after oxidative thermal cycling indicates severe degradation of these materials under these particular conditions.

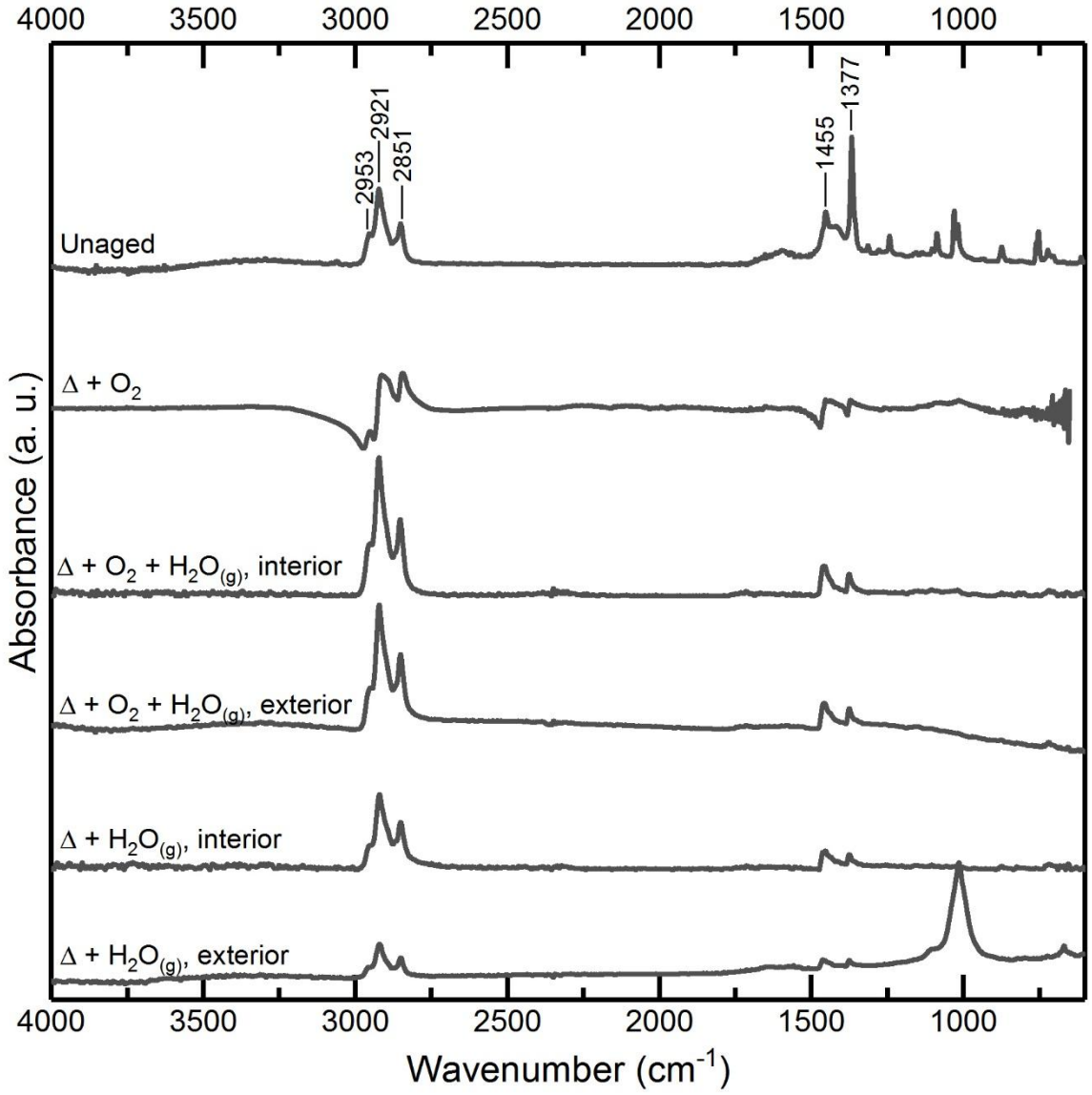

Figure 2. ATR-FTIR spectra of EPDM O-rings aged under the listed conditions; data were shifted vertically for clarity.

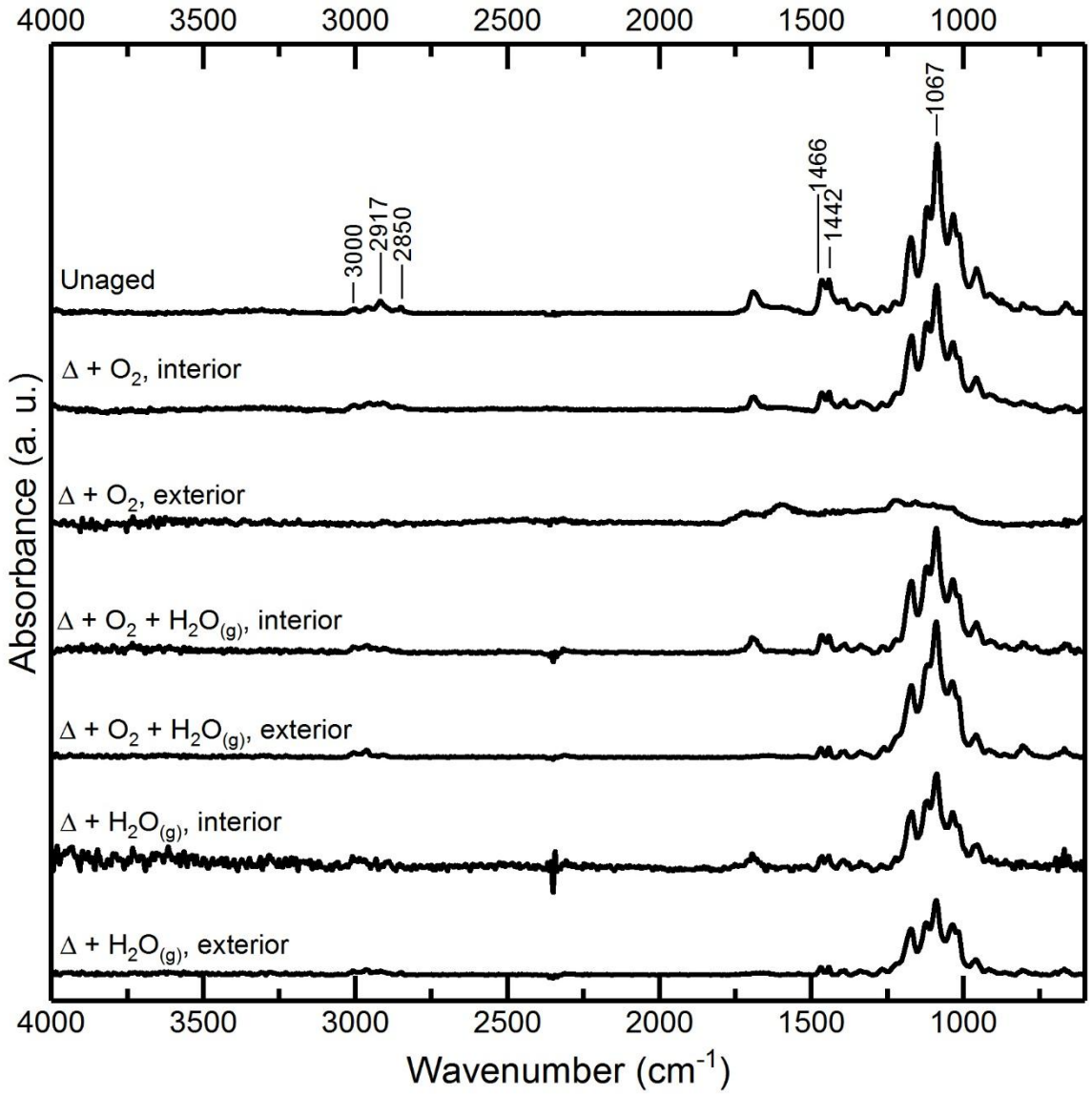

Figure 3. ATR-FTIR spectra of FEPM O-rings aged under the listed conditions; data were shifted vertically for clarity.

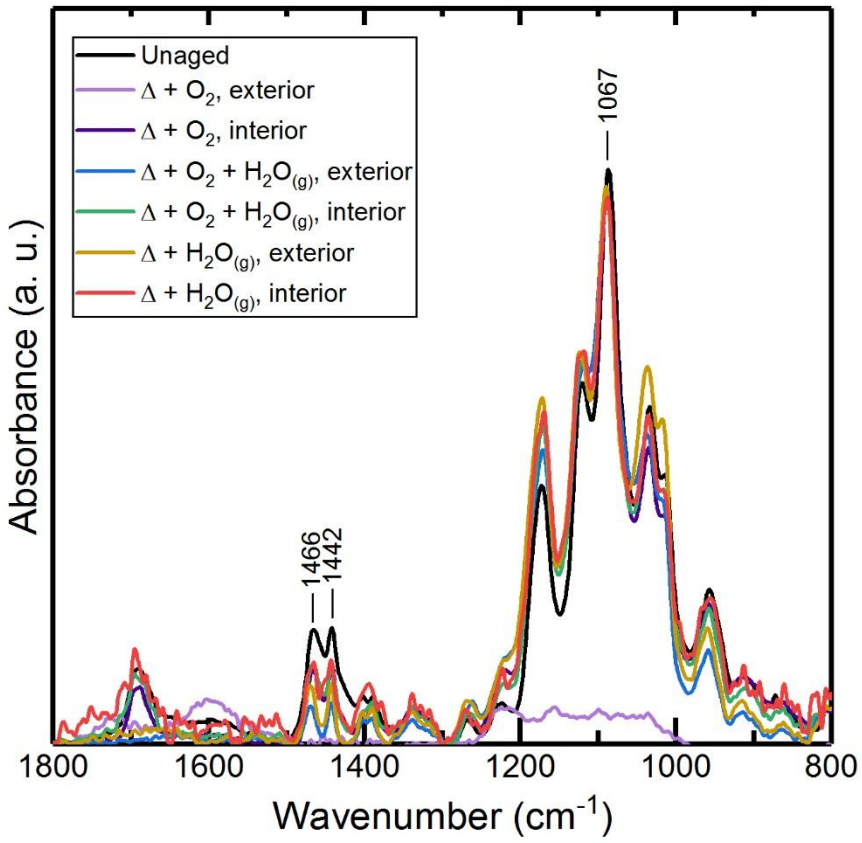

Figure 4. Highlighted area of the ATR-FTIR spectra of FEPM O-rings aged under the listed conditions. Spectra were normalized to the 1067 cm^{-1} peak of the unaged material.

The combination of large O-ring cross-sectional diameter with the very high exposure temperatures (300°C) suggest that DLO may be present in the oxidatively aged samples. Since spectral quality using FTIR spectroscopy was low, another way to assess DLO effects is using a modulus profiling apparatus to probe changes in modulus across the sample cross-section. For example, an increase in modulus can suggest crosslinking reactions have occurred while a reduction in modulus may be due to more chain scission. Figure 5 shows modulus profile data for EPDM and FEPM under the three aging conditions. EPDM experienced edge hardening

under both steam conditions, with the sample exposed to oxygen having a larger increase in modulus at the edges[1]. FEPM showed significant edge hardening (around 1 mm on each edge) after exposure to elevated temperature in air, but little change when aged in the presence of steam. Clearly, DLO has occurred when aging these O-rings, and the extent to which DLO is anticipated for the materials is estimated later.

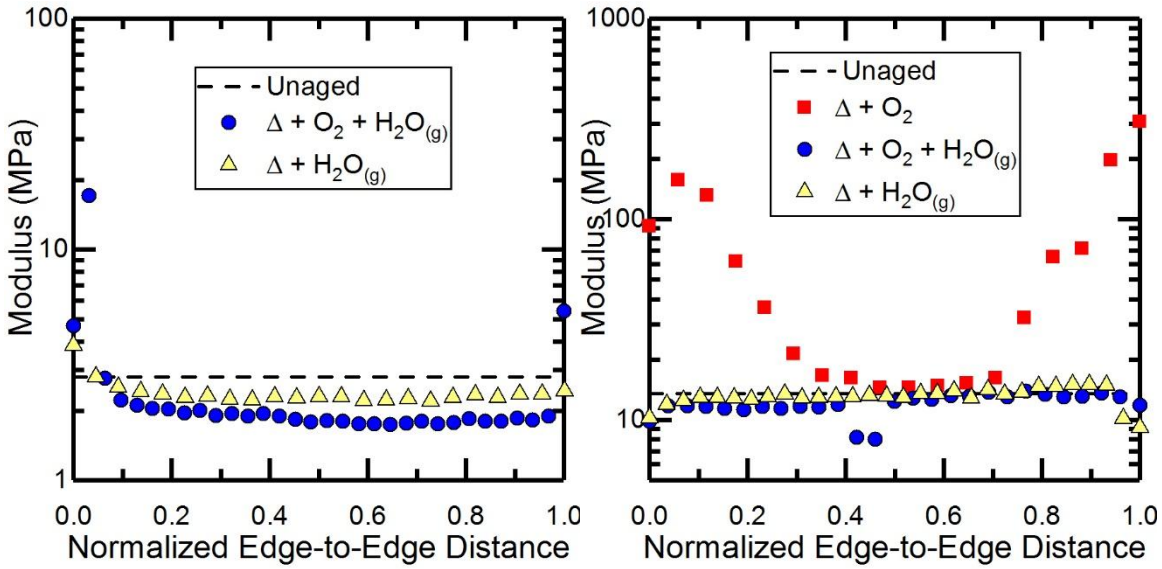

Figure 5. Modulus as a function of edge-to-edge distance of aged EPDM (left) and FEPM (right).

Elucidation of oxidative versus hydrolytic degradation sensitivity and the role of DLO was carried out using ultrasensitive oxidation experiments. For these measurements, each material was cut into pieces with thicknesses of approximately one millimeter or less in an effort to minimize DLO interference with the measurements. Around 0.1 g of elastomer was sealed in an ampoule, backfilled with air having a known concentration of oxygen, and placed into an oven at 125, 150, 175, and 200°C. Temperatures above 200°C were not investigated, due to the

[1] Note that EPDM which endured the thermo-oxidative exposure was not analyzed because it was reduced to a powder and is therefore not shown.

inevitable occurrence of DLO for even thin sample thickness and short exposure times [24, 25]. Four to five data points were taken at each temperature and averaged; Figure 6 displays these results as well as oxidation rates for an additional, unfilled EPDM material [26], and its filled counterpart [15]. All EPDM materials had similar activation energies (c.a. 105 kJ/mol), whereas the E_a for FEPM was lower (~80 kJ/mol).

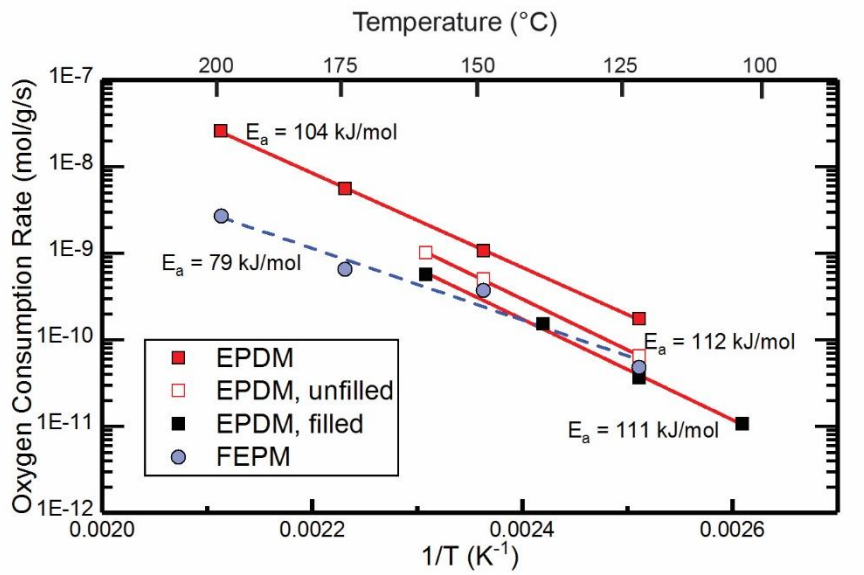

Figure 6. Arrhenius plot of oxygen consumption rates for EPDM and FEPM, in comparison with previously examined unfilled black EPDM [26] and its filled version [15]. Activation energies are also listed.

Measuring oxidation rates is an easy approach to rate the oxidation sensitivity of a material and is also a critical parameter for the assessment of potential DLO effects [24, 25]. Using the assumption that linear Arrhenius behavior is maintained when extrapolating to 300°C, an estimation of oxidation rates at this higher temperature can be attempted. For our EPDM and FEPM materials, oxidation rates at 300°C were estimated to be on the order of $7x10^{-6}$ and $7x10^{-7}$ mol/g/s, respectively. Despite the uncertainty in our extrapolation over such a large temperature range, we nevertheless anticipate that rates above $1x10^{-7}$ mol/g/s will likely be relevant.

These estimated oxidation rates, φ_{Ox}, along with oxygen permeability, P_{O2}, can be used to estimate whether or not diffusion limited oxidation (DLO) will be of concern [24, 27]. DLO arises when the rate of diffusion of oxygen into the sample is slower than the rate of oxidation; therefore, samples will age faster at the outer surfaces than the interior. The critical length scale above which non-homogeneous aging is expected to occur for two-sided oxidation, the L_{c90}, can be calculated for a given temperature. Oxygen permeability at 300°C is estimated to be $1x10^{-7}$ ccSTP/cm/s/cmHg for EPDM [28] and $9x10^{-7}$ ccSTP/cm/s/cmHg for FEPM[2] [29]. L_{c90} is then calculated using these estimated values for oxidation rates and oxygen permeability along with Equation 2 [30, 31] listed below.

$$L_{c90} = \sqrt{\frac{\alpha(\beta+1)*p*P_{O2}}{\varphi_{Ox}*22400*\rho}} \qquad \textbf{Equation 2}$$

where p is the partial pressure of oxygen (at sea level and 300°C ≈ 31 cm Hg), P_{O2} is oxygen permeability, φ_{ox} is oxidation rate, and ρ is the density of the polymer (EPDM ≈ 1.2 g/cc, FEPM ≈1.7 g/cc). This equation depends on beta (i.e. the partial pressure dependence of oxidation rate) and alpha (a relative thickness term). Under normal thermo-oxidative conditions and assuming beta =1, Eq. 2 can be simplified to yield approximate L_{c90} estimations with Eq. 3 [32].

$$L_{c90} = \sqrt{\frac{2*p*P_{O2}}{\varphi_{Ox}*22400*\rho}} \qquad \textbf{Equation 3}$$

[2] Calculated for polytetrafluoroethylene.

The L_{c90} for EPDM and FEPM under atmospheric conditions at 300°C was thus calculated to be 6 and 50 µm, respectively. Since the original test involved thermal cycling, these values may not accurately reflect the actual oxidation conditions for the O-ring exposures in the original experiments. Changes in permeability and oxidation rates are significant enough at lower temperatures that the actual Lc_{90} value could be larger. Nevertheless, from a purely oxidation point of view, the approximately 5 mm diameter O-rings aged in this study will be subject to severe diffusion limited oxidation behavior at these high aging temperatures. The L_{c90} is the approximate thickness for which nearly homogenous (90% homogeneity) aging is expected when both surfaces have access to oxygen. However, when significant DLO applies and the oxidation becomes surface limited, e.g. when thick specimens with surface oxidation are considered, there may be more of an interest to predict the depth of an oxidized layer. Since an oxidized layer does not have a specific maximum depth, but rather shows a transition zone into the material, it results in a mathematical description which is not straightforward. An oxidized layer is often defined as the depth to which 90% of all oxidation occurs. For most practical purposes, an L_{c90} is somewhat similar to an "oxidation depth" and can offer basic estimations. As the L_{c90} thickness is used to characterize two-sided oxidation, it is intuitive that the oxidation intensity for single sided exposure will drop off significantly over a given L_{c90} thickness, and the L_{c90} then represents approximately an oxidation layer depth.

To better understand the crosslinked state of the aged materials, an additional experiment was conducted in which a square piece of about 6 cm x 6 cm x 1 mm (L x W x T) thickness of each material was aged at 300°C in open air for 114 hours (Figure 7). Periodic sampling was carried out to measure weight loss. The test was done in Albuquerque, NM, USA which corresponds to P_{O2} of 18 kPa (2.55 psi) and is lower than the 41 kPa (6 psi) calculated for the uncompressed,

sealed oxidative environment experiments carried out at BNL where the aging anomaly was observed. EPDM showed the largest initial decline in weight but leveled off with approximately 80% weight retention. FEPM showed a more consistent decline, with about 75% of the material left after the aging was completed.

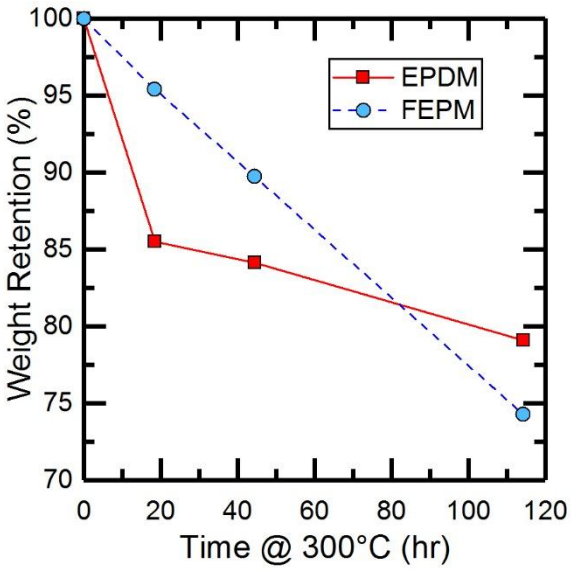

Figure 7. Percent weight retention as a function of aging time at 300°C. Lines are drawn as visual aids (solid for EPDM, dashed for FEPM).

These aged square specimens ($m_{initial}$) were then refluxed in p-toluene for 20 hours, weighed ($m_{swelled}$), then dried overnight at room temperature followed by additional drying for six hours at 90°C before being weighed a final time (m_{dried}). Solvent uptake factor was determined by dividing $m_{swelled}$ by $m_{initial}$ and gel content by dividing m_{dried} by $m_{initial}$. The results of this experiment are shown in Table 5. Changes between the unaged uptake factor and % gel content to the aged specimens can indicate the occurrence of crosslinking or chain scission reactions. For example, in crosslinking, the material would become denser and making it more difficult for solvent to penetrate into the polymer. In a similar fashion, increased crosslink density would lead

to less material loss when exposed to solvent; in other words, gel content would increase. EPDM had a decrease in solvent uptake factor, indicative of crosslinking. Unfortunately, EPDM becomes very brittle during oxidative aging at 300°C; small pieces of material flaked off and made it impossible to obtain an accurate final dried weight, hence the gel content of the aged EPDM is not reported. FEPM also showed evidence of crosslinking with a minor decrease in solvent uptake factor and increase in gel content.

Table 5. Solvent uptake factor and gel content for unaged EPDM and FEPM as well as results for those materials aged 114 hours at 300°C in air.

	EPDM		*FEPM*	
	Unaged	Aged 114 hr @ 300°C	Unaged	Aged 114 hr @ 300°C
Solvent Uptake Factor	2.42 ± 0.06	1.18 ± 0.08	1.50 ± 0.02	1.41 ± 0.09
% Gel Content	88.6 ± 0.2	*	97.0 ± 0.1	97.4 ± 0.2

**This value was not calculated for aged EPDM due to some material loss after refluxing in solvent.*

Up to this point, none of our analyses indicated any particularly unusual trends, except for the initial visual observation (Table 3) of FEPM and EPDM remaining intact after aging under thermo-oxidative + hydrolytic conditions. Again, it was highly unexpected that this dual-aging environment would somehow minimize the oxidative sensitivity of the two elastomers. In an effort to validate the initial observation, we conducted another carefully controlled experiment where EPDM was aged under thermo-oxidative and thermo-oxidative + hydrolytic conditions.

For both aging experiments, approximately 0.2 g of a 3.5 mm diameter EPDM O-ring (70 Duro Black) was added to a 46 cm^3 pressure vessel and aged for 22 hr at 240°C. The steam exposure also contained 1 cm^3 of water which was sufficient for generating a steam equilibrium with some liquid water at the aging temperature. In addition, the sample in the hydrolytic and oxidative environment was suspended using a wire to prevent submersion in the water. Under these conditions, both EPDM samples experience a p_{O2} of approximately 30 kPa (4psi) at 240°C.

Upon completion of the aging experiment, it was noted that the $\Delta + O_2 + H_2O_{(g)}$ sample was more flexible (by general handling observation) than the $\Delta + O_2$ material. However, surface cracking was noted on the sample aged with steam that was not present on the sample aged without steam (Figure 8). The $\Delta + O_2 + H_2O_{(g)}$ sample was also slightly swollen compared to the $\Delta + O_2$ sample (~ 0.03 mm difference in O-ring diameter).

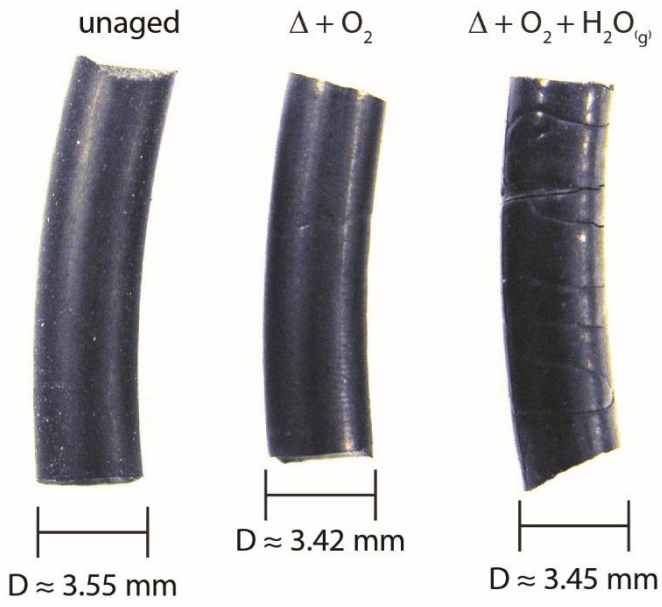

Figure 8. Unaged EPDM (left), EPDM aged in air at 240°C (middle), and EPDM aged in

air and steam at 240°C.

As DLO is anticipated in this aging experiment at 240°C, modulus profiles were taken of these and the original O-rings that were aged at 300°C. To accurately capture the edge hardening effect, data points were taken every 20 µm to create a high resolution scan of the edge area up to a distance of 180 µm (Figure 9). Two important trends are apparent in this plot: First, water does not appear to participate in any adverse degradation phenomenon (yellow triangles) – modulus remains relatively unchanged for the sample aged in the thermo-hydrolytic environment at 300°C. Second, and more unexpectedly, increasing temperature appears to increase the oxidation inhibition effect of water. More specifically, the sample aged at 300°C for 120 hours (dark blue diamonds) had less edge hardening than the sample aged at 240°C for 22 hours (light blue circles). In addition, the L_{c90} value for EPDM at 300°C was estimated to be 6 µm. Clearly, these 3.5 mm thick samples are showing evidence of DLO, as predicted.

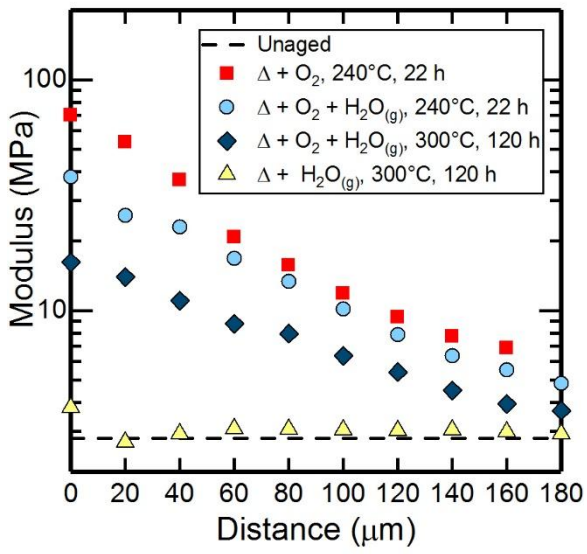

Figure 9. High resolution edge scan of EPDM O-rings aged under thermo-oxidative (red squares) and thermo-oxidative + hydrolytic (light blue circles) conditions at 240°C and with thermo-oxidative + hydrolytic (dark blue diamonds) and thermo-hydrolytic (yellow triangles) exposure at 300°C. The presence of water reduces oxidative degradation trends while the steam environment in itself does not result in any material changes.

Until now, the 70 Duro Black EPDM was the specific material under review. This lead to the immediate question whether or not the observed trend was specific to that formulation and/or filler(s), or if it was true of EPDM in general. Thus, we exposed two additional EPDM formulations, one carbon black (CB)-filled and one unfilled, to 240°C for 22 hours. Figure 10 shows modulus profiles taken from the edge to 600 μm into the approximately 2.5 mm thick by 5.5 mm wide samples. These data clearly show edge hardening under thermo-oxidative conditions for both EPDMs. The unfilled EPDM had no change in modulus under thermo-oxidative + hydrolytic exposure, whereas the filled sample had edge hardening but to a lesser extent than in the purely oxidative case. Furthermore, the filled EPDM clearly shows hardening from the edge up to approximately 500 μm depth (Figure 10, right) after oxidative aging, but this modulus increase is only to 100 μm depth when steam is present. These values are significantly higher than the 6 μm predicated as an L_{c90} of EPDM at 300°C. This value was estimated after extrapolating oxidation rates and oxygen permeability from 200 – 300°C, which is a rather significant projection. Either or both of these assumed linear extrapolations could be inappropriate, or some type of mechanistic change may occur over that temperature range that we did not anticipate, thus having our prediction diverge from what was experimentally observed. It highlights the challenge in predicting material lifetimes and aging behaviors when

DLO participates at high temperatures. Finally, the steam anomaly was visually apparent when examining the unfilled, white (i.e. no carbon black filler) EPDM; the oxidative aging shows a more prominent color change gradient and larger depth of color change than the oxidative + hydrolytic exposure (Figure 11).

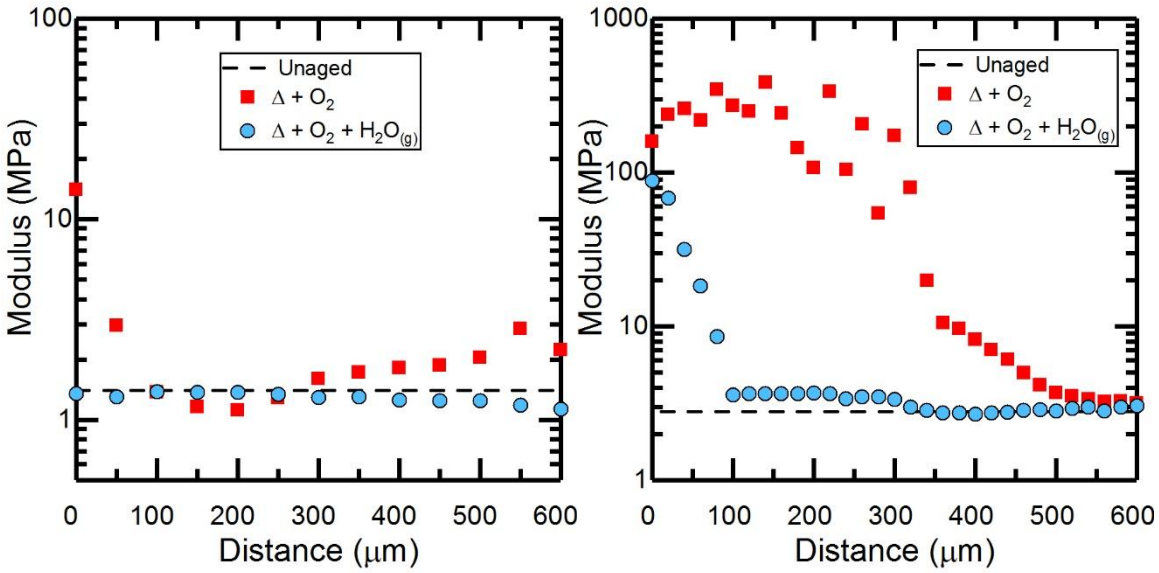

Figure 10. Modulus of (left) unfilled and (right) CB-filled EPDM rubbers as a function of distance. These profiles reflect scans of the sample edges, not through the entire cross-section.

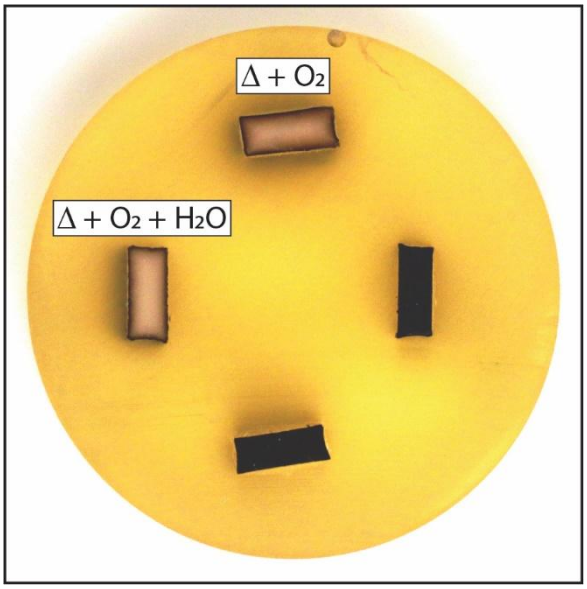

Figure 11. Photograph of EPDM aged at 240°C for 22 hours under thermo-oxidative (top) and thermo-oxidative + hydrolytic conditions (right). Also shown are the filled EPDM materials – thermo-oxidative (bottom) and thermo-oxidative + hydrolytic (left). Samples are embedded in an epoxy and were used for modulus profile testing.

At this point, evidence suggests that water does interfere with thermo-oxidative degradation and that it is only minorly formulation specific. However, exactly how the water inhibits oxidative damage is unclear. For instance, Figure 9 may suggest a lower oxidation rate, as less edge hardening is observed in the presence of steam (less oxidative crosslinking). However, this does not rule out the possibility that steam exposure may counteract hardening (extra crosslinking) through additional hydrolytic damage for which the unaged material is not immediately susceptible, or that results in mechanistic changes. Hydrolytic sensitivity in the presence of oxidative damage would also be consistent with the observed lower moduli for the combined steam/oxidative/300°C condition. The modulus profiles for the filled EPDM (Figure 10, right) could also be interpreted with a change in oxygen permeability, with a lower O_2 permeability in

the presence of steam. This is evident as a lower penetration depth of the hardening effect (i.e. a shallower degradation process). In fact, a change in oxygen permeability in the presence of water has been documented for some polymers [33-35]. Furthermore, permeability can also be affected by polymer morphology (e.g. semi-crystalline versus amorphous) as well as hydrophilicity [33-35].

Aside from the likely changes in oxidation rate and oxygen permeability, Garton [36] and coworkers have shown some evidence of a pH dependence on the impact of water on thermo-oxidative degradation; the authors investigated the oxidation of polyolefins in aqueous media and found that under acidic conditions an inhibition effect of water on oxidation was observed, whereas under neutral or basic pH oxidation was accelerated. The authors suggested that this behavior was related to the decomposition of hydroperoxides and subsequent formation of peroxy anions – peroxy anions can perform a nucleophilic attack of hydroperoxides to form radical intermediates that contribute to degradation. Acidic conditions prevent the creation of peroxy anions by stabilizing hydroperoxides and thus reduce oxidative degradation. Contrarily, neutral to basic environments have the opposite effect and contribute to accelerated oxidation. In the case of EPDM and FEPM, acidic conditions associated with dissolved water in the polymer are anticipated due to acidic degradation products as well as from potential hydrofluoric acid elimination (in the case of the fluoropolymer). Therefore, the observed inhibition effect of water on thermo-oxidative degradation may be linked to the underlying behavior of hydroperoxides. It is clear that we are not currently in position to fully describe the root cause of this anomalous behavior. At the same time, we expect that a combination of factors (changes in oxidation rate and O_2 permeability under steam conditions, additional sensitivity to hydrolytic damage, and

mechanistic changes in relation to hydroperoxides) will likely act in parallel to result in these material behaviors.

4. Conclusions

An aging anomaly of EPDM and FEPM was noted in our previous screening study of elastomers [1]; namely, both materials showed visible signs of degradation following thermo-oxidative conditions but maintained integrity under thermo-hydrolytic and thermo-hydrolytic plus thermo-oxidative conditions. Other than the visual inspection of the materials aged at 300°C, no unexpected behavior was apparent in oxidation rates, modulus profiles (presence of DLO), weight loss behavior (TGA, solvent swelling), or chemical changes (FTIR). An additional aging study under thermo-oxidative ($\Delta + O_2$) and thermo-oxidative plus hydrolytic ($\Delta + O_2 + H_2O$) was carried out at 240°C to validate the original findings. Interestingly, EPDM once again showed that steam reduces oxidative degradation levels (as observed through modulus changes) in the O-ring material. Even more surprisingly, this inhibition effect seems to be amplified as temperature is increased. In addition, it was shown that the effect of steam was not limited to one specific EPDM formulation – three different formulations showed the same trend. A combination of chemical and physical property changes in the presence of steam, such as oxidation rate and O_2 permeability changes, additional sensitivity to hydrolytic damage, as well as mechanistic changes in relation to hydroperoxides, may act in parallel and result in these unusual material degradation behaviors. Overall, these studies show that EPDM and FEPM O-rings may actually offer some limited performance at high temperatures in the presence of steam. Assuming that sealing force is maintained, EPDM could be a cost-effective alternative to some higher priced fluoroelastomers used in high temperature aqueous environments.

5. Acknowledgements

The authors would like to thank Douglas Blankenship for funding assistance. We would also like to thank Douglas Brunson, Avery Cashion, David Chavira, Grzegorz Cieslewski, Steve Knudsen, and Mark Grubelich for assistance with experimental setup and execution, and for use of their laboratory space.

This publication was based on the work supported by the Geothermal Technologies Office in the US Department of Energy (DOE) Office of Energy Efficiency and Renewable Energy (EERE), under the auspices of the US DOE, Washington, DC, under Contract No. DE-AC02-98CH 10886.

Sandia National Laboratories is a multimission laboratory managed and operated by National Technology and Engineering Solutions of Sandia, LLC, a wholly owned subsidiary of Honeywell International, Inc., for the U.S. Department of Energy's National Nuclear Security Administration under contract DE-NA0003525.

6. References

1. Sugama, T., Pyatina, T., Redline, E.M., McElhanon, J.R., and Blankenship, D., *Degradation of different elastomeric polymers in simulated geothermal environments at 300 °c.* Polym Degrad Stab, 2015. **120**: p. 328-339.
2. Sugama, T., *Surface analyses of fluoroelastomer bearings exposed to geothermal environments.* Mater Lett, 2001. **50**: p. 66-72.
3. Sugama, T. and Sullivan, B., *Hydrothermal oxidation of fluoroelastomer bearings after a year-long exposure to geothermal environments.* J Mater Sci Lett, 2001. **20**(18): p. 1737-1740.
4. Mitra, S., Ghanbari-Siahkali, A., Kingshott, P., Almdal, K., Rehmeier, H.K., and Christensen, A.G., *Chemical degradation of fluoroelastomer in an alkaline environment.* Polym Degrad Stab, 2004. **83**(2): p. 195-206
5. Embury, P., *High-pressure gas testing of elastomer seals and a practical approach to designing for explosive decompression service.* Sealing Tech, 2004. **June**: p. 6-11.
6. Silverman, S.A., Bhavsar, R., Edwards, C., Virally, S., and Foxenberg, W., *Use of high-strength alloys and elastomers in heavy completion brines*. 2003.
7. Endo, M., Noguchi, T., Ito, M., Takeuchi, K., Hayashi, T., Kim, Y.A., Wanibuchi, T., Jinnai, H., Terrones, M., and Dresselhaus, M.S., *Extreme-performance rubber nanocomposites for probing and excavating deep oil resources using multi-walled carbon nanotubes.* Adv Funct Mater, 2008. **18**: p. 3403-3409.
8. Rogers, J., *Achieving rgd resistance to meet current oilfield needs.* Sealing Tech, 2011. **October** p. 9-12.
9. Lin, C.-W., Chien, C.-H., Tan, J., Chao, Y.-J., and Zee, J.W.V., *Dynamic mechanical characteristics of five elastomeric gasket materials aged in a simulated and an accelerated pem} fuel cell environment.* Int J Hydrogen Energy, 2011. **36**(11): p. 6756-6767.
10. Tan, J., Chao, Y.J., Yang, M., Williams, C.T., and Van Zee, J.W., *Degradation characteristics of elastomeric gasket materials in a simulated pem fuel cell environment.* J Mater Eng Perform, 2008. **17** (6): p. 785-792
11. Bernstein, R. and Gillen, K.T., *Predicting the lifetime of fluorosilicone o-rings.* Polym Degrad Stab, 2009. **94**: p. 2107-2113.
12. Gillen, K.T., Bernstein, R., and Wilson, M.H., *Predicting and confirming the lifetime of o-rings.* Polym Degrad Stab, 2005. **87**: p. 257-270.
13. Gillen, K.T., Celina, M.C., and Bernstein, R., *Validation of improved methods for predicting long-term elastomeric seal lifetimes from compression stress–relaxation and oxygen consumption techniques.* Polym Degrad Stab, 2003. **82**: p. 25-35.
14. Gillen, K.T., Celina, M.C., and Keenan, M.R., *Methods for predicting more confident lifetimes of seals in air environments.* Rubber Chem Technol, 2000. **27**: p. 265-283.
15. Gillen, K.T., Celina, M.C., Clough, R.L., Malone, G.M., Keenan, M.R., and Wise, J., *New methods for predicting lifetimes in weapons. Part 1: Ultrasensitive oxygen consumption measurements to predict the lifetime of epdm o-rings*. 1998, Sandia National Laboratories.
16. Delor, F., Teissedre, G., Baba, M., and Lacoste, J., *Ageing of epdm - 2. Role of hydroperoxides in photo- and thermo-oxidation.* Polym Degrad Stab, 1998. **60**: p. 321-331.
17. van Duin, M., Orza, R., Peters, R., and Checkik, V., *Mechanism of peroxide cross-linking of epdm rubber.* Macromol Symp, 2010. **291-292**: p. 66-74.
18. Harwood, H.J., *Ethylene-propylene-diene monomer (epdm) and fluorocarbon (fkm) elastomers in the geothermal environment.* J Test Eval, 1983. **11**: p. 289-298.

19. Wise, J., Gillen, K.T., and Clough, R.L., *An ultrasensitive technique for testing the arrhenius extrapolation assumption for thermally aged elastomers.* Polym Degrad Stab, 1995. **49**: p. 403 - 418.
20. Assink, R.A., Celina, M., Skutnik, J.M., and Harris, D.J., *Use of a respirometer to measure oxidation rates of polymeric materials at ambient temperatures.* Polymer, 2005. **46**: p. 11648 - 11654.
21. Gillen, K.T., Clough, R.L., and Quintana, C.A., *Modulus profiling of polymers.* Polym Degrad Stab, 1987. **17**: p. 31-47.
22. Petrovic, Z.S. and Zavaro, Z.Z., *Reliability of methods for determination of kinetic parameters from thermogravimetry and dsc measurements.* J Appl Polym Sci, 1986. **32**: p. 4353-4367.
23. Budrugeac, P. and Segal, E., *The application of the thermogravimetric analysis (tga) and of the differential thermal analysis (dta) for rapid thermal endurance testing of electrical insulating materials.* An Univ Bucuresti Chimie, 2005. **I-II**: p. 241-246.
24. Celina, M.C., *Review of polymer oxidation and its relationship with materials performance and lifetime prediction.* Polym Degrad Stab, 2013. **98**: p. 2419-2429.
25. Celina, M.C., Dayile, A.R., and Quintana, A., *A perspective on the inherent oxidation sensitivity of epoxy materials.* Polymer, 2013. **54**(13): p. 3290 - 3296.
26. Celina, M.C., *Unpublished data for unfilled black epdm material*.
27. Gillen, K.T., Bernstein, R., and Celina, M.C., *Challenges of accelerated aging techniques for elastomer lifetime predictions.* Rubber Chem Technol, 2015. **88**: p. 1-27.
28. Celina, M.C. and Gillen, K.T., *Oxygen permeability measurements on elastomers at temperatures up to 225°c.* Macromolecules, 2005. **38**(7): p. 2754-2763.
29. Pasternak, R.A., Christensen, M.V., and Heller, J., *Diffusion and permeation of oxygen, nitrogen, carbon dioxide, and nitrogen dioxide through polytetrafluoroethylene.* Macromolecules, 1970. **3**(3): p. 366-371.
30. Gillen, K.T. and Clough, R.L., *Rigorous experimental confirmation of a theoretical model for diffusion-limited oxidation.* Polymer, 1992. **33**(20): p. 4358 - 4365.
31. Gillen, K.T., Wise, J., and Clough, R.L., *General solution for the basic autoxidation scheme.* Polym Degrad Stab, 1995. **47**: p. 149-161.
32. Clough, R.L. and Gillen, K.T., *Oxygen diffusion effects in thermally aged elastomers.* Polym Degrad Stab, 1992. **38**: p. 47-56.
33. Gavara, R. and Hernandez, R.J., *The effect of water on the transport of oxygen through nylon-6 films.* J Polym Sci, Part B: Polym Phys, 1994. **32**: p. 2375-2382.
34. Hu, Y.S., Mehta, S., Schiraldi, D.A., Hiltner, A., and Baer, E., *Effect of water sorption on oxygen-barrier properties of aromatic polyamides.* J Polym Sci, Part B: Polym Phys, 2005. **43**: p. 1365-1381.
35. Auras, R., Harte, B., and Selke, S., *Effect of water on the oxygen barrier properties of poly(ethylene terephthalate) and polylactide films.* J Appl Polym Sci, 2004. **92**(3): p. 1790-1803.
36. Henry, J.L., Ruaya, A.L., and Garton, A., *The kinetics of polyolefin oxidation in aqueous media.* J Polym Sci, Part A: Polym Chem, 1992. **30**: p. 1693-1703.